To be published in Optics Letters:

Title: Helical Distributed Feedback Fibre Bragg Gratings &Rocking Filters in 3D Printed Preform-Drawn Fibre

Authors: John Canning,yitao wang,Matthieu Lancry,Yanhua Luo,GangDing Peng

Accepted: 21 August 20

Posted 24 August 20

DOI: https://doi.org/10.1364/OL.401081

Helical Distributed Feedback Fibre Bragg Gratings & Rocking Filters in 3D Printed Preform-Drawn Fibre

JOHN CANNING,[1,] YITAO WANG[1,2], MATTHIEU LANCRY[2], YANHUA LUO[3], GANG-DING PENG[3]*

[1]*interdisciplinary Photonics Laboratories (iPL), School of Electrical & Data Engineering, Tech Lab, UTS, Ultimo, Sydney NSW 2007*
[2]*Institut de Chimie Molecuaire et des Materiaux d'Orsay, Universite Paris Sud, Université Paris Saclay, Paris, France*
[3]*National Fibre Facility (NFF), UNSW, Randwick, Sydney NSW 2052, Australia*
**Corresponding author: John.Canning@uts.edu.au*

Received XX Month XXXX; revised XX Month, XXXX; accepted XX Month XXXX; posted XX Month XXXX (Doc. ID XXXXX); published XX Month XXXX

Using induced UV attenuation across a twisted fibre asymmetric core drawn from a 3D printed preform, linear fibre Bragg gratings are produced on one side of the core. By removing the twist, a helical grating with a period matching the twist rate is produced. Balancing the rate with the polarisation beat length in a form birefringent fibre allows the production of a combined rocking filter and fibre Bragg grating device with tunable properties. Direct observation of the fibre grating dispersion within the rocking filter rejection band is possible.

http://dx.doi.org/10.1364/OL.99.099999

By pre-twisting a birefringent fibre it is possible to balance and match optical losses of each polarisation eigenstate creating an effective zero birefringence. In this way, phase shifted gratings can in principle be written that have no intrinsic splitting, a method previously utilised to remove intrinsic birefringence in conventional photosensitive rare-earth doped germanosilicate optical fibres for optimized distributed feedback (DFB) fibre lasers [1,2]. Notably, it was a simple method to remove polarisation hole burning and subsequent laser instability that arises from intrinsic form birefringence existing in all fibres. Those results demonstrated the principle worked well with commercial-ready CW 244 nm laser writing of fibre Bragg gratings (FBG). Despite the weakly absorbed CW 244 nm light generally producing very little intrinsic birefringence ($\Delta n < 10^{-6}$, depending on [GeO_2]), it is commensurate with existing form birefringence in uniform low loss fibres. The small but finite induced twisting is thought to arise predominantly from defect and/or interfacial stress anisotropy [cal] be used to compensate weak form birefringence directly. This allows permanent birefringence removal from grating devices with untwisting.

The method was instrumental in the successful demonstration of ultra-narrow linewidth DFB fibre lasers. In this work, we go further to demonstrate the novel production of helical gratings in fibres that have higher form birefringence arising from an initial strong core asymmetry combined with the greater induced index asymmetry from pulsed UV light.

Penetration across a germanosilicate core using pulsed 193 nm [3,4] is significantly less than at 244 nm for reasons that involve two-step excitation paths [5]. At higher intensities, these lead to localized index change at the core cladding interfaces that can generate, within a uniform fibre, significant form birefringence compared to UV CW light. This can be exploited by matching the twist rate with the induced birefringence beat length such that it makes both eigenstates degenerate through cross-coupling, then the twist period, Λ_τ (>> Λ_B) will be superimposed and locked onto the grating with Bragg period, Λ_B, after the fibre twist is relaxed or removed. Under such a condition, it should be possible to produce a long period rocking filter [6,7] superimposed on the grating profile – its 1st order (m = 1) spectral position is then related to the wavelength, λ, dependent birefringence $B(\lambda)$:

$$\lambda = \Lambda_\tau B(\lambda) \quad (1)$$

Figure 1 summarizes the concept. It can be greatly enhanced using a pre-existing high asymmetry in the fibre core profile.

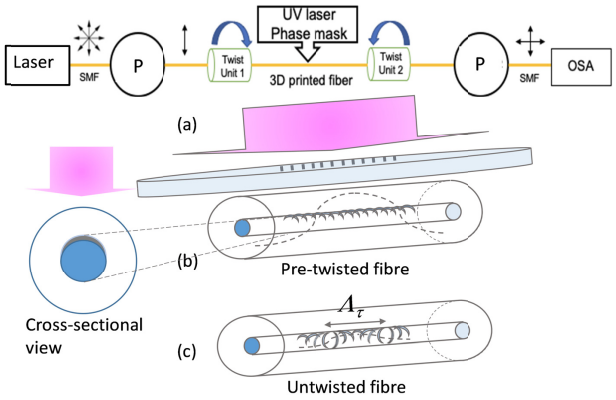

Fig. 1. A schematic of the grating writing (a) in twisted fibre with a twist period, Λ_τ. Closeup is shown in (b), along with the subsequent untwisting of the fibre (c). The untwisted grating has a period equal or close to Λ_τ. The cross-section shows the localised index change critical for efficient cross-coupling after twisting is removed (SMF: singlemode fibre; OSA: optical spectrum analyser; P: polariser).

$$\Delta n \sim \sqrt{\frac{B_g}{0.32}} = 0.0038 \qquad (2)$$

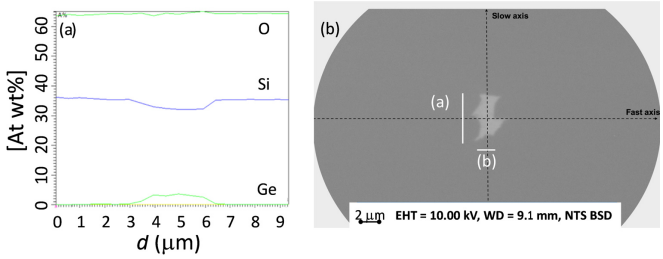

Fig. 2. Analysis of a highly asymmetric germanosilicate fibre drawn from a 3D printed preform: (a) X-ray analysis (EDX) of composition showing A% of O, Si and Ge; (b) SEM micrograph showing approximate long (a) and short axes (b). The fibre is treated like an elliptical fibre in the first instance, ignoring the jagged profile that gives rise to scattering loss.

The highly asymmetric core optical fibre (Fig. 2) was produced by additive manufacturing [8-10]. In short, this single mode optical fibre was drawn from a preform prepared by 3D printing with a nanoparticle/photocurable resin preparation, subsequent core formation, thermal debinding to remove the polymer, and finally consolidation and drawing of the preform into fibre on an optical fibre draw tower. It has a germanosilicate core and silica cladding, both dopant distributions shown in Figure 2(a) along one axis of the fibre. These were measured by energy dispersive X-ray analysis (EDX) in a scanning electronic microscope (SEM - ZEISS SUPRA 55 VP). About 8 at. wt% of Ge is found in the core, the rest is silica. No evidence of residual polymer or water from the resin preform is detected suggesting, within resolution, a pure germanosilicate fibre has been produced. The highly asymmetric fibre core arises from core distortion during drawing and is ideal for this work. The photosensitivity is as expected for a germanosilicate fibre, qualitatively similar to commercial fibres [11]. The printed preform was not uniform leading to stresses that distorted the softer germanosilicate core producing the observed twisted elliptical shape (long axis $\phi \sim 4$ μm, short axis $\phi \sim 1.3$ μm; they are not orthogonal). This shape was observed along the length of fibre and gives rise to scattering losses of $\alpha \sim 0.24$ dB/cm, measured by cutback. It is likely that there is also cross polarisation mixing occurring both from a frozen in twist variation and natural twisting of the fibre.

Two major axes are shown in Figure 2(b). Assuming orthogonal eigenstates, the form or geometric birefringence is estimated from interference measurements to be $B_g \sim \Delta n_{a,b} \sim 4.5 \times 10^{-6}$. From this figure, if the core is approximated as an equivalent elliptical fibre core one can estimate the core/cladding index from [12], if the fibre axes ratio of a/b ≥ 3, then $B_g \sim 0.32(\Delta n)^2$. Rearranging accordingly:

If the fibre eigenstates are twisted sufficiently, then further modal mixing and overlap will occur leading to degeneracy of the two eigenstates. Loss will also be degenerate but further twisting will break that degeneracy. This in turn generates high quality, narrower and stronger spectral profiles since polarisation eigenstates are overlapping. In previous work, phase-shifted gratings were used to demonstrate high finesse correction of the weak form birefringence within standard fibres, making it suitable for active DFB fibre lasers to remove polarisation competition and mode beating [1,2]. Here, twisting the fibre is used to compensate for the form or shape-induced birefringence caused by the high asymmetry of the fibre. By writing a highly localized uniform grating directly into this twisted fibre using the strong attenuation described above, the release of the fibre results in a unique twisted grating helix around the core over the grating length with twist period Λ_τ that counters the birefringence in that region. Uniform gratings (L = 1 cm) were produced by direct writing with 193 nm [13] are used (Ar F laser: λ = 193 nm, w = 15 ns, repetition rate RR = 10 Hz, fluence f_{cum} = 360 J/cm^2).

In physically twisting the grating, as sought $\Lambda_\tau >> \Lambda_B$. With appropriate selection to phase match the index difference between polarization eigenstates as described above, direct polarization coupling can be achieved such that one state is coupled into the other. The spectral bandwidth over which this occurs is determined by the period and length of interaction. This is effectively a rocking filter as described by equation (1) [6,7,14]. Since this is on top of the Bragg filter itself, the spectral filter of the rocking filter can be tuned to sit directly over the Bragg filter.

The combined rocking and Bragg grating filter produce an interesting function – whereas one polarisation can be coupled into another across a spectral bandgap to generate a finite rejection filter function, within that filter bandgap there will be a direct transmission of a narrower Bragg resonance of the same polarisation. This is because the

Bragg grating dispersion destroys the phase matching condition of the rocking filter function around its bandgap. A similar phenomenon was exploited in novel integrated transmission pass photonic bandgap waveguides where the dispersion of a silicon-on-silica photonic crystal played a similar role [15] and in a tapered silica-on-silicon multimode waveguide [16].

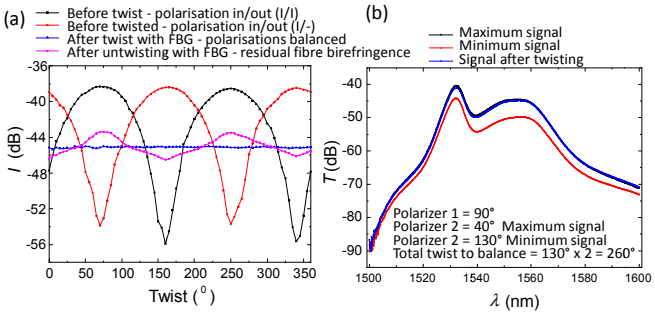

Fig. 3. (a) Polarised transmission with the rotation angle. Black is the case where the output and input polarisers are aligned, whereas red is the case where they are orthogonal; and (b) Er^{3+} -doped fibre amplifier transmission spectra through the 3D printed fibre. More information on fibre polarisation can be found here [12,17].

The experimental setup shown in Figure 1(a) was used to characterise twisting and polarisation. Two rotational twist mounts were used to twist the fibre before grating writing. The polarization mixing between eigenstates occurs for one polarisation over the fibre sample length [12,17]. During the test, the initial measurement is made for one parallel input polarisation at 360^0 and then repeated for orthogonal input at 90^0 from the initial state. The shift in spectral fringes of the parallel and orthogonal polariser shown in Figure 3(a) measures the birefringence. The depth of the signal background reflects differences in scattering loss for each eigenstate. The fibre is twisted in both directions (blue line shown in Figure 3(a)). When twisted $\theta \sim 130^0$ in each fibre direction ($\Delta\theta \sim 5.2^0$ /cm), the polarisation eigenstates are fully mixed and the response is a flat line. Assuming perfectly orthogonal eigenstates, the rocking filter bandwidth lies in the near IR window. Twisting separates the elliptical eigenstates and shifts the spectrum, demonstrating ready tunability. The twist is approaching 260^0. The transmission spectra in Figure 3(b) also shows a similar result. After twisting, the maximum fibre signal coincides with the minimum signal.

The weaker undulating line in Figure 3(a) demonstrates that the pre-twist can permanently lock-in a helical spiral of index change arising from the twisting of the photosensitive induced index changes when the fibre twist is removed. An estimate of the amount locked in, or reduced, after twist is removed is $\Delta(\Delta B) \sim 85\%$; better optimisation should lead to 100%. This points to substantial counter birefringence induced by the localised UV changes at the asymmetric core-cladding interface which are now helically distributed along the grating (Figure 1(c)). Importantly, this result shows that utilizing strong pulsed UV attenuation when grating writing within this fibre drawn from a bottom-up 3D printed preform has similar properties to standard commercial photosensitive fibre.

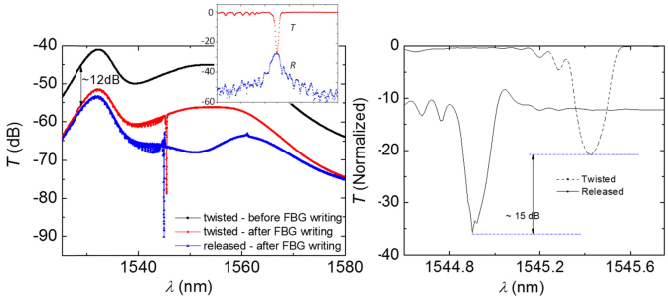

Fig. 4. (a) Transmission spectra of the 3D printed fibre with the FBG inscribed by an ArF exciplex laser; (b) Comparison with and after removing applied twist. Inset shows transmission and reflection of a grating written with no polarisers and no twist [11] for comparison.

The spectral fringe has weakened sharply after the fibre twist was removed. It has not vanished completely suggesting the optimal twist has not been reached and/or some relaxation has occurred. The latter may be explained noting that the exposure itself, in addition to localised index changes, has altered the stress properties of the fibre and these play a role in contributing to the overall deviation from degeneracy observed before irradiation and release - i.e. optimal twisting has to take into account these changes in iterative optimisation. With an optimum twist angle, the grating is written with a UV laser. Once UV exposure is matched then the fibre can be relaxed and the asymmetry in the exposed region in theory lost.

Figure 4 shows the grating results in this fibre before and after the twist is released. An initial bulk exposure affects fibre transmission significantly with $\Delta\alpha \sim 20$ dB induced flat attenuation across the spectrum. This is attributed to enhanced Mie-like scattering of the grating out of the fibre because it is highly localized to one side, greatly exacerbating the losses arising from the non-adiabatic core shape. In uniform fibres, FBG attenuation due to scattering from off-centre exposed regions can be as high as $\alpha \sim 0.1$ dB/cm with writing at $\lambda = 193$ nm [4]. When the fibre twist is released the FBG peak shifts to shorter wavelengths by $\Delta\lambda \geq -0.5$ nm, indicating the fibre was under a small tensile load during writing. The grating becomes stronger with a narrowing of the 3dB bandwidth by $\Delta(\Delta\lambda) \sim 0.028$ nm or approximately a third.

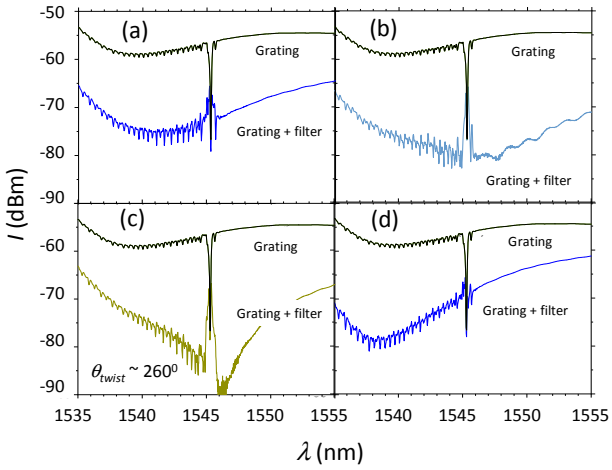

Fig. 5. By fine tuning the degree of twist in the setup shown in Fig. 1, the rocking filter can be shifted over the fibre Bragg grating bandgap to optimize the notch transmission peak to floor signal within the rocking filter rejection band - (a) to (b) to (c) to (d). When overlapping spectrally, this improves polarization cross-coupling around the transmission notch, including the side cladding mode grating resonances at shorter wavelengths, and demonstrates tunability. This is due to the phase spoiling the grating and side resonance dispersion profile introduces.

A large induced attenuation around the grating spectrum reflects high core asymmetry so that when unwound, the localised UV induced changes introduce a broadband, flat loss around the grating. This is a combination of the grating asymmetry along with grating twist as the fibre twist is relaxed, leading to a periodic coupling of the two polarization eigenstates – a rocking filter is superimposed on the Bragg grating. From equation (1), the central wavelength of this rocking filter is dependent on the twist period, Λ_τ, the coupling order, m, and the wavelength dependent birefringence $B(\lambda)$:

$$\lambda_\tau = \frac{\Lambda_t}{m} B(\lambda) \quad (3)$$

However, those wavelengths that interact with the fibre Bragg grating experience resonance delays, or a dispersive time, and therefore a phase delay so the condition in equation (3) is not met over the grating bandgap. At the point where the rocking filter phase matching is no longer achieved, the rocking filter cross coupling from one polarization to the other is avoided and the signal not blocked by the in-line polarizers. This leads to a transmission peak notch within the rocking filter bandwidth, shown in more detail in Figure 5. Similarly, this behavior is observed at the shorter wavelength Bragg cladding resonances. Further, it predicts that there should be no transmission peak in the centre of the fibre grating and cladding resonances because there is no dispersion at that point – and this is observed as an narrow rejection notch within the transmission band. What this physically means is that there is a rocking filter induced broad rejection band of one polarisation state and a narrower suppression of this polarisation rejection in the centre due to the fibre grating dispersion. An ultranarrow polarisation notch within the bandgap is also present – quite a complicated polarisation distribution in the spectra is created with a relatively simple grating combination. This can be extended by designing complex fibre Bragg grating functions such as chirped gratings, sample gratings and more.

Figure 5(c) shows when the rocking filter spectrum exactly overlaps the FBG spectrum. Further optimization in both signal-to-noise and rocking filter bandwidth can be locked in once the ideal conditions are implemented initially. When the rocking filter and Bragg grating wavelengths, λ_τ, λ_B are equal:

$$\lambda_\tau = \lambda_B = 2n\,\Lambda_B = \frac{\Lambda_t}{m} B(\lambda) \quad (3)$$

Rearranging for the lowest rocking filter order m = 1 and minimizing the twist over Λ_τ = 1 cm to obtain full rotation, the minimum birefringence, $B(\lambda)$, can be estimated:

$$B(\lambda) = \frac{2\bar{n}\Lambda_B}{\Lambda_\tau} > 1.45 \times 10^{-4} \quad (4)$$

Given the presence of cross-coupling increases with twist before degeneracy, this figure is a measure of elliptical birefringence. As it approaches or exceeds the UV induced index change for the fibre grating, elliptical birefringence will convert to circular birefringence. As well as form twist, it combines localised UV-induced changes making it > 20 times the estimated untwisted fibre form birefringence. The value will also be larger than UV induced birefringence generated by 193 nm written gratings within uniform fibres [18].

The observed resonances are asymmetric reflecting the grating chirp and consequently the asymmetric time delay on the grating band edge. This resonant phenomenon is difficult to directly observe in spectra because of the presence of uncoupled background light. Coupling between polarisation states with the rocking filter and using the Bragg grating dispersion to spoil that coupling, has been used to generate a transmission notch within a high loss polarisation window. Combining these unique filter properties opens up interesting filter functions that offer narrowband fibre grating transmission and selective narrow and broadband polarisation separation around the FBG bandgap. Such devices could be used in advanced polarisation discrimination and polarisation based filtering applications in telecommunications and sensing. Further they offer a novel dispersion diagnostic because the information revealed by in-line analysis of the resonance impacted polarisation states directly mirrors the fibre grating dispersion. By comparison, conventional approaches to measuring dispersion use a network analyser whilst modulating a narrow linewidth source sufficiently fast to obtain high resolution group delay measurements after signal processing. The current approach is also an alternative to direct bandgap resonance measurements from the side that rely on low levels of scattered light that limits resolution [19].

In conclusion, it has been shown within germanosilicate fibres produced from 3D printed preforms that it is possible to overcome polarisation splitting from form birefringence by twisting and to undo this permanently by as much as 85% with laser processing. Hybrid rocking filter and fibre Bragg

grating devices where high-resolution selective spoiling of the rocking filter polarisation coupling by the Bragg grating dispersion are demonstrated. This enables novel polarisation and helical filter profiles to be tailored within the rejection band by directly tailoring the fibre Bragg grating. More localized multiphoton excitation of the glass band-edge with femtosecond near IR lasers [20,21], if needed, may permit additional degrees of processing and tunability.

Acknowledgements. Y. Wang acknowledges training and assistance with direct grating writing from Kevin Cook.

Funding. Private funds supporting this work are acknowledged. Y. Wang acknowledges support from the PHC- FASIC (French-Australia Science Innovation Collaboration Grants) program.

The authors declare no conflicts of interest.

References

1. A. Michie and J. Canning, Postdeadline, Aust. Conf. Optical Fibre Tech. (ACOFT), Sydney, Australia, (2002).
2. J. Canning, A. Michie, Australian Provision Patent, PS2846 (2001); A. Graf, A. Michie, G. Edvall, J. Canning and M. Englund, PCT/AU2003/000728, WO2003/104869 (2002).
3. A. M. Vengsarkar, Q. Zhong, D. Inniss, W. A. Reed, P. J. Lemaire, and S. G. Kosinski, Opt. Lett., **19** (16), 1260-1263 (1994).
4. M. Janos, J. Canning and M.G. Sceats, Opt. Lett., 21 (22), 1827, (1996)
5. J. Canning, Opt. Fibre. Tech, **6**, 275-289, (2000).
6. R. H. Stolen, A. Ashkin, W. Pleibel, and J. M. Dziedzic, Opt. Lett. **9** (7), 300-302 (1984).
7. D. C. Johnson, F. Bilodeau, B. Malo, K. O. Hill, P. G. J. Wigley, and G. I. Stegeman, Opt. Lett., **17** (22), 1635-1637 (1992).
8. Y. Chu, X. Fu, Y. Luo, J. Canning, Y. Tian, K. Cook, J. Zhang and G-D. Peng, Opt. Lett. **44** (21), 5358 -5361, (2019).
9. K. Cook, J. Canning, S. Leon-Saval, Z. Redi, Md. Hossain, J-E. Comatti, Y. Luo and G-D. Peng, Opt. Lett. **40** (17), 3966-3999, (2015).
10. K. Cook, G. Balle, J. Canning, L. Chartier, T. Athanze, M.A. Hossain, C. Han, J-E. Comatti, Y. Luo and G-D. Peng, Opt. Lett., **41** (19), 4554-4557, (2016).
11. K. Cook, J. Canning, Y. Luo, and G-D. Peng, "Confirmation of 193 nm photosensitivity in germanosilicate fibre drawn from a 3D printed preform" Unpublished (2019); Reported in J. Canning, "Smart Sensing", UTS Smart Sensing Research Showcase, NSW Smart Sensing Network (NSSN), (2020)
12. A. Kumar and A. Ghatak, Polarization of Light with Applications in Optical Fibres, SPIE Press Book, TT90, (2011).
13. J. Canning, M.G. Sceats, H.G. Inglis and P.Hill, Opt. Lett., **20** (21), 2189-2191 (1995).
14. Retu Kaul, Opt. Lett. **20** (9), 1000-1001 (1995).
15. J. Canning, M. Kristensen, N. Skivesan, C. Martelli, A. Tetu and L.H. Frandsen, J. Europ. Opt. Soc., **4**, 09019, (2009).
16. J. Canning and D. Moss, Opt. Lett., **23** (3), 174-176, (1998).
17. R. Hui and M. O'Sullivan, Fibre Optic Measurement Techniques, Academic Press, (2009), ISBN 978-0-12-373865-3
18. T. Erdogan and V. Mizrahi, J. Opt. Soc. Am. B., **11** (10), 2100-2105, (1994).
19. J J. Canning, M. Janos, D Stepanov and M.G. Sceats, Electron Lett. **32** (17), 1608 – 1610 (1996)
20. A. Martinez, M. Dubov, I. Khrushchev and I. Bennion, Electron. Lett. **40** (19), 1170 – 1172, (2004)
21. Technicasa White Paper (2019), https://technicasa.com/technologies-high-temperature-fibre-bragg-grating-fbg-sensors/

Full citation listings

[1] A. Michie and J. Canning, "Properties of a twisted DFB fibre laser", Postdeadline, Aust. Conf. Optical Fibre Tech. (ACOFT), Sydney, Australia, (2002).
[2] J. Canning, A. Michie, "Helical feedback laser operation in a linear DFB laser", PS2846 (2001); A. Graf, A. Michie, G. Edvall, J. Canning and M. Englund, "Helical feedback structures", PCT/AU2003/000728, WO2003/104869 (2002).
[3] A. M. Vengsarkar, Q. Zhong, D. Inniss, W. A. Reed, P. J. Lemaire, and S. G. Kosinski, "Birefringence reduction in side-written photoinduced fiber devices by a dual-exposure method", Opt. Lett., **19** (16), 1260-1263 (1994).
[4] M. Janos, J. Canning and M.G. Sceats, "Incoherent scattering in optical fibre Bragg gratings", Opt. Lett., 21 (22), 1827, (1996)
[5] J. Canning, "Photosensitisation and photostabilisation of laser-induced index changes in optical fibres", Opt. Fibre. Tech, 6, 275-289, (2000).
[6] R. H. Stolen, A. Ashkin, W. Pleibel, and J. M. Dziedzic, "In-line fiber-polarization-rocking rotator and filter," Opt. Lett. **9** (7), 300-302 (1984).
[7] D. C. Johnson, F. Bilodeau, B. Malo, K. O. Hill, P. G. J. Wigley, and G. I. Stegeman, "Long-length, long-period rocking filters fabricated from conventional monomode telecommunications optical fiber", Opt. Lett., **17**(22), 1635-1637 (1992).
[8] Y. Chu, X. Fu, Y. Luo, J. Canning, Y. Tian, K. Cook, J. Zhang and G-D. Peng, "Silica optical fibre drawn from 3D printed preforms", Opt. Lett. 44, 21, 5358 -5361, (2019).
[9] K. Cook, J. Canning, S. Leon-Saval, Z. Redi, Md. Hossain, J-E. Comatti, Y. Luo and G-D. Peng, "Air-structured optical fibre drawn from a 3D-printed optical preform", Opt. Lett. **40** (17), 3966-3999, (2015).
[10] K. Cook, G. Balle, J. Canning, L. Chartier, T. Athanze, M.A. Hossain, C. Han, J-E. Comatti, Y. Luo and G-D. Peng, "Step-index optical fibre drawn from 3D printed preforms", Opt. Lett., **41** (19), 4554-4557, (2016).
[11] K. Cook, Y. Luo, J. Canning and G-D. Peng, "Confirmation of 193 nm photosensitivity in germanosilicate fibre drawn from a 3D printed preform", Unpublished (2019); Reported in J. Canning, "Smart Sensing", UTS Smart Sensing Research Showcase, NSW Smart Sensing Network (NSSN), (2020)
[12] A. Kumar and A. Ghatak, Polarization of Light with Applications in Optical Fibres, SPIE Press Book, TT90, (2011).
[13] J. Canning, M.G. Sceats, H.G. Inglis and P.Hill, "Transient and permanent gratings in phosphosilicate optical fibres produced by the flash condensation technique", Opt. Lett., **20**(21), 2189-2191 (1995).
[14] R. Kaul, "Pressure sensitivity of rocking filters fabricated in an elliptical-core optical fiber," Opt. Lett. **20** (9), 1000-1001 (1995).
[15] J. Canning, M. Kristensen, N. Skivesan, C. Martelli, A. Tetu and L.H. Frandsen, "Spectrally Narrow Polarisation Conversion in a slow-light photonic crystal waveguide", J. Europ. Opt. Soc., **4**, 09019, (2009).
[16] J. Canning and D. Moss, "Grating-based transmission bandpass filters using dispersion matched mode conversion", Opt. Lett., 23, (3), 174-176, (1998).
[17] R. Hui and M. O'Sullivan, Fibre Optic Measurement Techniques, Academic Press, (2009), ISBN 978-0-12-373865-3
[18] J. Canning, M. Janos, D Stepanov and M.G. Sceats, Electron Lett. **32** (17), 1608 – 1610 (1996)
[19] T. Erdogan and V. Mizrahi, "Characterisation of UV-induced birefringence in photosensitive Ge-doped silica optical fibres", J. Opt. Soc. Am. B., 11 (10), 2100-2105, (1994).
[20] A. Martinez, M. Dubov, I. Khrushchev and I. Bennion, "Direct writing of fibre Bragg gratings by femtosecond laser", Electron. Lett. **40** (19), 1170 – 1172, (2004)
[21] K. Cook, J. Canning, S. Bandyopadhyay, M. Lancry, C. Martelli, T. Jin and A. Csipkes, "Technologies for high temperature fibre Bragg grating (FBG) sensors", Technicasa White Paper (2019), https://technicasa.com/technologies-high-temperature-fibre-bragg-grating-fbg-sensors/